Further Results of Grossversuch IV: The Effect of the First Rocket Launched into a Potential Hail Cell

J. BADER

Atmospheric Physics ETH, Zurich, Switzerland

W. A. STAHEL

Seminar of Statistics ETH, Zurich, Switzerland

W. SCHMID

Atmospheric Physics ETH, Zurich, Switzerland

(Manuscript received 19 February 1991, in final form 21 August 1991)

ABSTRACT

The data obtained in Grossversuch IV about hail prevention triggered the hypothesis that only the first rocket launched into a potential hail cell decreases hail kinetic energy in an effect-time interval around 10 min after launching time. Several variations of a randomization test were applied to substantiate this hypothesis. All showed a tendency to confirm the hypothesis, the most significant result being a p value of 0.2%. However, since the test was applied to the data that had been explored to generate the hypothesis, the significant result should be interpreted as a strong hint rather than as a statistical proof.

1. Introduction

The hail-suppression experiment Grossversuch IV was designed to test for effects of a specific prevention technique on hail kinetic energy. Days with a potential of hail storms were randomly assigned to the treatment or the control group. Each cell that fulfilled a criterion derived from some synoptic and radar measurements was seeded with silver iodide by rockets. The response variable was the logarithm of each cell's hail kinetic energy as estimated from PPI radar measurements. No significant effect of seeding was found for this response variable [for details, see Federer et al. (1978/79, 1986)].

The extensive measurements taken during the experiment allowed for more detailed studies of any effects of the treatment on the development of the cells, even if a global effect on hail energy was not found. Waldvogel and Schiesser (1985) examined the effect of launching a rocket on the subsequent estimates of hail kinetic energy. Again, no significant effect was found. A more refined analysis by Schiesser et al. (1992) showed a (formally) significant increase. The main results of Grossversuch IV made it clear that beneficial effects of seeding, if any, would be plausible only for small cells. (This became clear from studying the dependence of the estimated seeding effect on the cell's predicted size.) A possible explanation for such a tendency suggests that the first (few) rocket(s) launched into a cell would be beneficial, whereas later rockets would increase hail energy (or aftereffects of the first rockets might be malicious if the cell survived).

In order to study such hypotheses, the lifetime of each of the 19 largest cells of the treatment group is subdivided into 10 equally long periods, Δt_k, $k = 1, 2, \cdots, 10$. For the rockets fired within these periods into "seeded" cells, the logarithmized values of estimated kinetic energy flow was obtained for a time interval from 10 min before to 20 min after the rocket was fired. Figure 1 shows the respective median curves for all seeded cells in the classes 1–4 and compares it with the corresponding curves for the 18 largest unseeded cells for which launching times were simulated by random numbers (see below for a precise description). Indeed, the first and second classes show an indication of a beneficial effect of seeding around and prior to 10 min after seeding. Adverse effects appear for later stages of development. They could be caused by immediate effects of the respective rockets or by aftereffects of earlier ones. The latter seems plausible since the diagrams for later periods do not show any pattern similar to a time point of largest effects.

In the remainder of this paper, some variations of a statistical test for examining the effect of the first rocket

Corresponding author address: Dr. Juerg Bader, Atmospheric Physics ETH, Honggerberg HPP, CH-8093 Zurich, Switzerland.

are described (section 2). These randomization tests avoid two pitfalls. First, correlations of effects of rockets within the same cell would invalidate usual randomization tests applied to all seeding events (rockets). Second, the selection of cells should not be based on total energy as done in Fig. 1, since this quantity can be influenced by seeding (even if statistically insignificantly), and the interpretation of significant results would be difficult. While the results of these tests show some formally significant effects (section 3), the reader should keep in mind that a test has been applied here to examine a hypothesis obtained from the same dataset after a considerable amount of exploration. Some physical interpretations of the statistical results are presented in section 4.

2. The test

a. *The response variable*

Let us first define the quantities used in Fig. 1. The area within a given cell where the plan position indicator (PPI) radar reflectivity at time t is between $z-1$ and z dbZ is $A_z(t)$. The hail energy flow is estimated by

$$E^{(z)}(t) = 5 \times 10^{-6} \sum_{z' \geq z} 10^{0.084 z'} A_{z'}(t) \qquad (1)$$

(Federer et al. 1978/79). Let

$$R^{(z)}(t, \Delta t) = \log[1 + \sum_{\tau=t}^{t+\Delta t-1} E^{(z)}(\tau)]. \qquad (2)$$

Throughout the manuscript, the time t means actual time minus "start time" t_0 of the cell. The start time is the time when the seeding criterion is fulfilled for the first time inside the experimental area. Let σ_{ij} be the time when the jth rocket is launched into cell i (on a treatment day).

The solid line in the first frame of Fig. 1 shows $\text{median}_{i,j}\,[R_i^{(61)}(\sigma_{ij}+\tau, 1)]$, as a function of $\tau = -10, -9, \cdots, 19$. Here the median is taken over all i, j for which cell i is seeded and has total energy $\sum_t E_i^{(Gr)}(t) > 1$ GJ; and $\sigma_{ij} \leq (t_{f,i} - t_{0,i})/10$, $t_{0,i}$ and $t_{f,i}$ are the start and end times of cell i. [The gradual version $E_i^{(Gr)}$ of E, defined in Federer et al. (1986), had been used to select the large cells in other preliminary studies.] For unseeded cells, randomly simulated launching times were used. The simulation method is described in Schiesser et al. (1992). Several specifica-

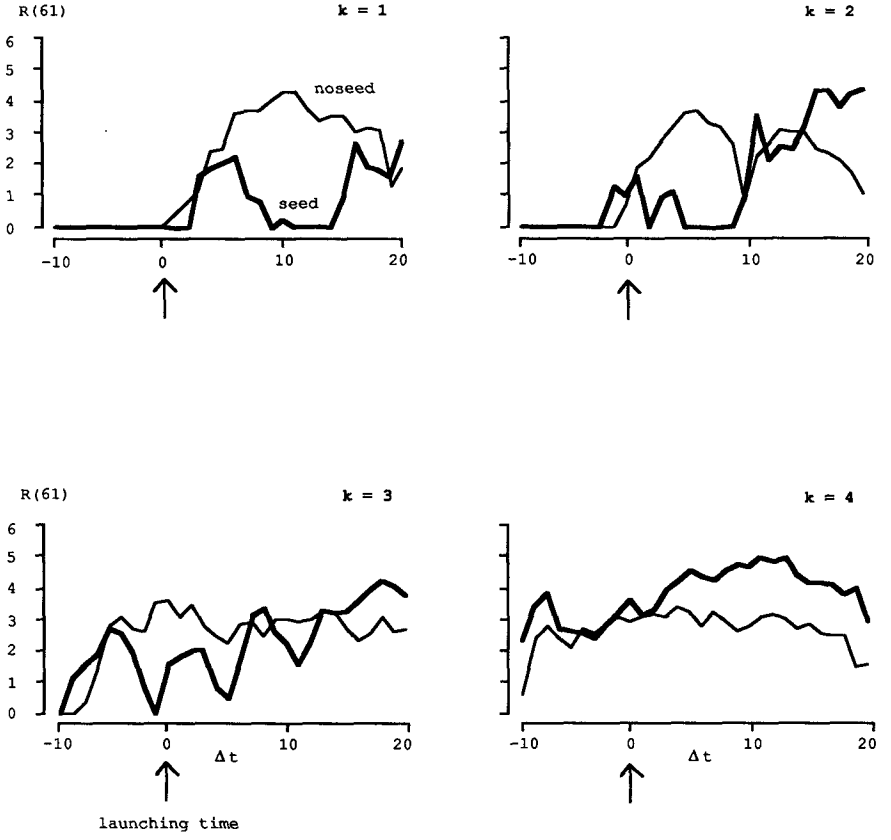

FIG. 1. Median curves of 19 seeded (thick line) and 18 unseeded hail cells for the time classes $k = 1$ to 4; Δt is the time difference to the rocket's launching time.

tions of this informal analysis are debatable, including those mentioned above. The idea of this paper is to present a more carefully designed analysis.

b. *Effect-time energy*

In this analysis, only the first rocket launched into each cell is examined. Let its launching time be σ_i instead of σ_{i1} for brevity. The working hypothesis is that the first rocket diminishes $R_i(t,1)$ during the "effect-time" interval $[\sigma_i + 1 + \Delta t_d, \sigma_i + 1 + \Delta t_d + \Delta t_e]$; Δt_d is called the delay time. Schiesser et al. (1992; Table 2) calculated suitable values Δt_d for some of the cells based on physical analyses of PPI and range–height indicator (RHI) sections of characteristic hail cells. Most results were between 5 and 10 min. The same values for all cells were used here and the results for Δt_d = 5, 8, and 10 min and Δt_e = 5, 10, and 15 min are given. The response variable is

$$Y_i(s) = R_i^{(61)}(s + 1 + \Delta t_d, \Delta t_e) \qquad (3)$$

with $s = \sigma_i$. It will be compared between seeded and unseeded cells below.

c. *Blocking*

Since small cells in this study behave differently from large ones, blocking on the basis of predicted size was applied. More specifically, the logarithm of the measured hail energy $E^{(56)}$, integrated over the time interval $[t_0 + 1, t_0 + 30]$, was predicted on the basis of information available at t_0 by the predictor function

$$\hat{R}^{(56)}(1, 30) = 0.422 \log[E_0^{(56)} + 0.01] + 0.402\mathrm{ZM}_0 - 18.839, \quad (4)$$

where $E_0^{(56)}$ is given by (1) for $t = t_0$ and $z = 56$, and ZM_0 is the maximal reflectivity at time t_0. This function is a slightly improved version of earlier ones (Federer et al. 1986). The squared multiple correlation was R^2 = .72. A prediction of $R^{(56)}$ was preferred to one of $R^{(61)}$, since the latter is zero for more than half of the observations. The cells were then ordered according to descending predicted size $\hat{R}^{(56)}$ (Table 1). Then blocks were formed by inspection to include, as a rule, n_{1b} = 2 seeded cells and a variable number n_{0b} of unseeded ones. Since there have been fewer seeded cells than

TABLE 1. Overview of hail cells originating within the test area, sorted by predicted energy.

i	Date	Cell	Seed	Block	$\hat{R}^{(56)}(t_0 + 1, 30)$	σ	SC*	$Y_i(\sigma_1)$	$Y_i(\sigma_2)$	$Y_i(\sigma_3)$
1	30 May 1979	1558	1	1	10.894	−1	0.5	7.748	7.689	*8.152*
2	8 August 1981	1710	1	1	9.946	9	1.0	4.691	*5.211*	5.214
3	6 August 1981	2006	1	1	9.707	5	0.5	*7.800*	7.776	6.646
4	31 May 1978	1227	0	1	9.463	—	—	3.672	3.914	2.563
5	7 August 1979	1851	0	1	9.273	—	—	7.287	5.782	7.586
6	10 June 1979	1337	1	2	9.258	2	0.5	7.977	*8.298*	—
7	1 June 1978	1833	0	2	9.065	—	—	8.197	7.865	—
8	18 July 1978	1206	0	2	8.988	—	—	9.005	7.084	—
9	12 July 1979	2044	0	2	8.650	—	—	7.078	7.274	—
10	15 July 1982	1452	1	2	8.585	10	1.0	*0.000*	0.000	—
11	5 June 1979	1709	0	3	8.309	—	—	5.908	5.880	—
12	3 June 1981	1950	1	3	8.216	2	1.0	4.683	*3.524*	—
13	29 July 1980	1427	0	3	7.814	—	—	6.507	6.820	—
14	6 August 1981	2043	1	3	7.568	4	1.0	*5.451*	5.915	—
15	31 May 1978	1428	0	3	7.558	—	—	5.661	5.686	—
16	8 August 1981	1505	1	4	7.555	3	1.0	2.532	*2.532*	—
17	10 June 1979	1302	1	4	7.490	−1	1.0	*2.000*	4.563	—
18	2 June 1979	1450	0	4	7.293	—	—	5.585	5.041	—
19	2 June 1979	1607	0	4	7.216	—	—	5.235	6.100	—
20	3 June 1981	2020	1	5	7.172	4	1.0	5.386	*5.386*	—
21	16 August 1978	1208	0	5	7.093	—	—	3.004	3.004	—
22	5 September 1978	1642	0	5	7.092	—	—	4.412	4.412	—
23	6 August 1979	1901	1	5	7.074	4	0.0**	*1.480*	1.480	—
24	24 June 1979	1930	0	5	7.038	—	—	2.556	2.556	—
25	7 August 1979	1804	0	5	6.976	—	—	4.559	4.559	—
26	5 September 1978	1917	0	5	6.928	—	—	3.440	3.440	—
27	14 September 1979	1437	1	6	6.720	4	1.0	2.921	*3.316*	—
28	14 September 1979	1355	1	6	6.707	5	0.5	*0.000*	0.000	—
29	21 May 1980	1842	0	6	6.428	—	—	3.880	3.955	—
30	5 June 1982	1323	0	6	6.344	—	—	0.000	0.000	—
31	5 September 1978	1814	0	6	6.290	—	—	4.699	4.699	—
32	21 May 1980	1657	0	6	6.266	—	—	0.000	0.000	—
33	15 June 1980	1420	0	6	6.242	—	—	1.944	2.563	—
34	31 May 1978	1351	0	6	6.171	—	—	3.924	3.968	—
35	31 July 1979	1612	0	6	6.171	—	—	5.575	5.321	—

* The seeding coverage SC is not used in this study.
** Cell 1901: those rockets were most probably shot in the downwind area.

unseeded ones in the experiment [due to various reasons, see Federer et al. (1986)], the average number of unseeded cells per block was 3.7, and no block had less than 2 such cells. It turned out that of the cells in blocks 7–27—those with low predicted hail energy—only a few produced a nonzero response regardless of treatment. These blocks are thus virtually useless for testing the hypothesis mentioned. They are dropped for what follows.

d. The test statistic

The n_{1b} (usually 2) seeded cells $j(b, k)$, $k = 1, \cdots n_{1b}$ in block b determine the same number of shooting times $\sigma_j(b, k)$. For example, for block $b = 4$, the first $n_{1b} = 2$ cells were seeded: $j(4, 1) = 16$ and $j(4, 2) = 17$. A rocket was shot into cells 16 and 17 3 min after ($\sigma = 3$) and 1 min before ($\sigma = -1$) their t_0, respectively. Using these times as potential seeding times for all cells i of block b, one obtains n_{1b} values $Y_i[\sigma_j(b, k)]$ of potential effect-time energy for each one of the $n_{0b} + n_{1b}$ cells in block b. For block 4, the potential effect-time energies $Y_i(\sigma)$ are evaluated for $\sigma = 3$ and $\sigma = -1$, and for all four cells $i = 16, 17, 18, 19$. These 4×2 Y values are listed in the columns $Y_i(\sigma_1)$ and $Y_i(\sigma_2)$ in Table 1. The test statistic T_b is the difference between the average of effect-time energies for the n_{1b} actual seeding events (italic values in Table 1) and for the remaining $n_{1b}(n_{0b} + n_{1b} - 1)$ potential ones ($T_4 = \frac{1}{2}(2.532 + 2.000) - \frac{1}{6}(2.532 + 4.563 + 5.585 + 5.041 + 5.235 + 6.100) = -2.577$). The Appendix describes how a randomization test within each block is constructed using this test statistic, and how these tests are combined to a global test.

e. Prediction

Different versions of the test are obtained by using a prediction for the potential effect-time energies on the basis of information on the development of the cell before the effect time. The prediction function obtained for $R^{(61)}(s + 9, 10)$ on the basis of all the $\sum_{b=1}^{6} n_{1b}(n_{0b} + n_{1b})$ potential seeding events was

$$\hat{R}^{(61)}(s + 9, 10) = -0.566 I_1 + 0.110 I_2 + 1.029 I_3 + 3.287 I_4 + 6.264 I_5 + 3.836 I_6 - 0.027\text{Dist} + 0.357 R^{(56)}(s - 4, 5) - 0.647 R^{(56)}(s + 1, 5) + 1.670\text{H0}, \quad (5)$$

where I_b is the indicator variable for block b ($I_b = 1$ for cells in block b and $I_b = 0$ otherwise), Dist is the distance of the cell from the radar station in kilometers (the beam has an elevation angle of 5°), and H0 is the height in kilometers of 0°C temperature. The R^2 value was .93. The residuals $Y_i'(s) = Y_i(s) - \hat{R}^{(61)}(s + 9, 10)$ were used instead of the $Y_i(s)$ values to perform an alternative randomization test. Note that the use of a prediction function in this way does not affect the validity of the randomization test, since no information about the actual randomization is used in the prediction.

A much simpler prediction function,

$$\hat{R}^{(61)}(s + 9, 10) = 4.321 + 0.0027 R^{(56)}(s - 9, 10), \quad (6)$$

with an R^2 of .44, is used in the same way as (5).

3. Results

Different tests with varying delay and effect times were carried out. In Table 2, one-sided p values are listed for the tests with five different combinations of delay- and effect-time duration. The results for an 8-min delay time and a 10-min effect time are the most significant, showing p values on the order of 1.5%–5%. The predictor functions do not increase the significance.

The variables used in the predictor functions (5) and (6) were tested in the same way in the spirit of comparing the baseline data. No significant differences turned up, but there was a tendency of higher values of $R^{(56)}(s + 1, 5)$ for seeded cells. This may help to explain why the use of predictor function (5) did not lead to more significant results.

As a kind of sensitivity analysis, Table 2 also shows the results for each block. The test statistics show a decrease of the logarithmized hail energy during the effect time for all test versions in blocks 2, 3, 4, and 6, whereas for block 1, which contains the biggest cells, an increase is indicated. No clear tendency is apparent in block 5. The smallest p values for all tests occur for blocks 3 and 4, suggesting that the seeding was most effective in these groups of hail cells. In view of the small number of cells, especially in these two blocks, the result should be interpreted with caution.

Note that in block 1, the three cells with the largest predicted energy had been seeded. Therefore, the results of tests based on blocks 2–6 have been included (Table 2). The results appear more significant (p values in the range 0.4%–2.6%) than those based on all the blocks.

From Table 2, one may also extract the dependence of the p values on the choice of the length and location of the delay- and effect-time intervals. Comparing the results of the tests with varying delay and effect times using no prediction, one concludes that the choice of 10-min effect-time duration 8 min after the rocket start appears optimal in detecting a possible seeding effect (compare also with Fig. 1, $k = 1$).

In Schiesser et al. (1992) the test using all rockets indicates an increase of the hail energy, contrary to the present results. One explanation is that seeding may influence the development of a hail cell first positively (decrease of hail) and then negatively, which means that the cell produces, as a whole, more hail than in the natural unseeded state. To check if there is an in-

TABLE 2. One-sided p values (%) of the within-block and global randomization test. First row is one-sided p values: (a) lower/upper for the within-block test; (b) lower for the global test. Second row is the value of the test statistic.

			Within-block test						Global test	
			Block						Blocks	
			1	2	3	4	5	6	2–6	1–6
			Number of randomizations							
Delay time	Effect time	Prediction	60	20	20	12	42	72	1000	1000
					(exact)				(sample)	
8	10	Eq. (5)	77/23	35/70	5/100	8/100	67/36	19/82	2.6	4.8
			0.77	−2.87	−1.17	−2.19	0.59	−0.84	−1.07	−0.81
8	10	Eq. (6)	90/12	35/70	10/95	8/100	40/62	24/78	0.4	1.6
			1.01	−2.60	−1.26	−2.62	−0.12	−1.10	−1.35	−1.01
8	10	—	92/10	35/70	5/100	5/100	40/62	22/79	0.2	1.5
			1.17	−2.66	−1.40	−2.58	−0.13	−0.81	−1.37	−1.01
8	5	—	83/18	30/75	5/100	25/83	64/38	42/60	17	27.2
			1.26	−1.67	−1.60	−0.82	0.59	−0.24	−0.59	−0.32
8	15	—	92/10	40/65	15/85	25/83	40/62	22/79	4.2	10.2
			1.18	−2.32	−0.25	−0.99	−0.19	−1.19	−0.96	−0.65
10	10	—	95/6	30/75	5/100	8/100	50/52	24/78	1.5	5.0
			1.29	−2.81	−0.87	−2.26	−0.06	−1.17	−1.28	−0.91
5	10	—	82/20	25/80	25/80	17/92	69/33	40/61	6.5	13.1
			0.95	−2.33	−0.98	−1.65	0.49	−0.73	−0.88	−0.62
Test for an increase after the effect time with response variable $R(t_0 + 24, 10) - R(t_0 + 9, 10)$:										
			21/80	85/20	65/40	100/8	90/14	79/29	0.7	1.5
			−0.67	2.36	1.14	2.77	3.34	−0.20	1.67	1.34

crease of the hail energy after the effect time, a further test is carried out and listed at the bottom of Table 2. A suitable test statistic is obtained as the difference of means of the response variable R for appropriate time intervals. Again, clear significance shows up for the simultaneous tests for an increase after the effect time, whereas the single-block p values are, at most, weakly significant.

4. Discussion

Although there are some strongly significant results, let us recall that these p values have to be interpreted with a grain of salt, since the tests were designed to check a phenomenon that was seen in the data after quite extensive searching for effects. Since the p values are rather low, these results should be considered to be a strong hint, but not proof, that the first rockets showed a beneficial effect in their effect-time interval. This beneficial action might be followed by an increase in hail energy afterwards. This would explain the adverse effects that appear in Fig. 1 for $k = 4$.

In the following, these statistical findings will be interpreted in terms of cloud microphysics and dynamics. This discussion must remain somewhat speculative at the present stage of our knowledge, since in situ measurements of the cloud particles within the analyzed storms are not available. However, measurements were made with a penetrating T28 aircraft through Swiss hailstorms in 1983 (Waldvogel et al. 1987). These measurements, together with indirect evidence about the physics of the Swiss-type hailstorms (radar data, collected hailstones), justify the following discussion. A comparison of our findings with a model simulation of a "seeded" hailcloud will also be given in this section.

a. Physical interpretation: Discussion of seeding hypotheses

The seeding hypothesis of Grossversuch IV was based on the existence of a so-called big-drop zone (BDZ), where the liquid water content is mainly concentrated in big supercooled raindrops. The BDZ was assumed to be located above −5°C within the environment of the main updraft. The seeding hypothesis states that the introduction of seeding material in the BDZ would produce a large number of efficient hail embryos that would compete for the liquid water (beneficial embryo competition), leading to more but smaller hailstones than would naturally occur (Waldvogel et al. 1987; Federer et al. 1978/79).

However, the mentioned T28 measurements showed practically no supercooled drops in that region at the time when seeding would be conducted. Waldvogel et al. (1987) found that there was already a large concentration of natural precipitating ice particles, but also a nonnegligible liquid water content that consists of cloud droplets or very small raindrops. Uncertainty exists about the representativity of these measurements for the cells used as the database for our statistics. Most

storms penetrated by the T28 were less intense (E_{GR} < 1 GJ) than the main part used in our test (E_{GR} > 1 GJ).

There is evidence that big drops occur in central European hailstorms in specific cloud regions.

- *Feeder clouds.* Meischner et al. (1991) found in a case study large differential radar reflectivities Z_{DR} in the feeder cloud of a squall line, which is an indicator for large drops. The radar reflectivity in feeder clouds is typically 20–25 dBZ, which is considerably smaller than the radar reflectivity in the BDZ of Grossversuch IV (above 45 dBZ). Meischner et al. inferred that a nearly monodisperse spectrum of large raindrops occured between the 12° and −3°C level in a low concentration. At the −5°C level ice is also occurring, but rain is still the dominant precipitation type. The warm cloud-base temperature and high vapor mixing ratio above the main inflow region of this squall line is an ideal condition for droplet growth by coalescence up to bigger raindrop sizes. The occurrence of large supercooled drops is a necessary condition for an efficient freezing with seeding material (see hypothesis above), which seems to be fulfilled at least sometimes in feeder clouds.
- *Main updraft region of large thunderstorms.* Indirect evidence for the occurrence of large supercooled drops in Swiss hailstorms has been obtained by analyzing hailstones collected from the ground in the experimental area. More than one-half had a frozen drop embryo, which, however, was often too big to be grown by coalescence and therefore was formed from melted and recirculated graupel or from liquid water that was shedded from the falling hailstones. Refer to Schiesser et al. (1992) for an extended discussion of that point. A recent case study of a multicell storm confirms these findings. Höller et al. (1991) concluded from radar measurements that large raindrops may also occur above freezing level around the main updraft region. They found zones of high Z_{DR} values, indicating large drops, at the boundary between the updraft and downdraft region (main precipitation core), sometimes reaching well above the freezing level and filling the vault region. They concluded from analyzing various radar-derived quantities that these large raindrops stem from melted graupel or hail.

In our opinion, the two situations given above do not match for the initial stage of the cells analyzed here when the first rocket reaches the target area. First, the target area is not located in the feeder cell (as in Farley's simulation, see below). Second, an extended recirculation of melted graupel as in the multicell case above is not likely to take place in this early stage.

Thus, the main conclusion is that big drops are not predominant in the target area of the first rocket, and therefore the Grossversuch IV seeding hypothesis cannot be a base for an explanation of the first rocket effect. Assume that the liquid water is mainly concentrated in cloud droplets or very small raindrops, according to the T28 aircraft measurements mentioned above. An explanation of our results can then be given by the following hypothesis: seeding considerably increases the number of ice crystals and therefore also increases the number of frozen cloud droplets, leading to an increased number of potential hail embryos. The resulting competition for the remaining liquid water leads to a slower growth of these embryos. Therefore, they reach the critical size for falling later, and the radar echo, measured below the seeding zone, becomes lower for a while. When the critical size is reached, more hailstones will fall, and this leads to an increased reflectivity.

Variations of such a hypothesis can easily be formulated. These results do not distinguish between them, and the above simple hypothesis is just one possible explanation.

One cannot assume that the hypothesis above is true for rockets started in the later stages of the storm. The increase of hail kinetic energy when testing all rockets, not only the first, as shown in Schiesser et al. (1992), is explained by an earlier freezing of recirculated melted graupel or shedded water due to seeding.

b. A comparison with a numerical simulation

There are several numerical modeling studies of hailstorms that also simulate seeding. The most recent and adequate study is that of Farley (1987). Farley simulated a multicellular hailstorm by a numerical cloud model that uses bulk microphysics with discrete graupel classes. He found an initially larger hail production in the seeded cases (AgI and mainly CO_2 seeding) 12 min (66 min simulation time) after seeding as compared to the natural case (Farley 1987). This feature is more pronounced in the CO_2 case than in the AgI case. After 3 min (69 min simulation time), the natural case has more hail aloft compared to the seeded cases, which have more hail near the ground. One can extract from Figs. 7 and 8 in Farley's article (contour plots of radar reflectivity for the natural and CO_2 seeded cases) similar curves for radar energy flow as shown in Fig. 1 based on the 45- and 50-dBZ contour lines (reference height 3000 m, only feeder cell). For the CO_2 case the radar energy flow occurs 3 min sooner than in the natural case. This is in agreement with the hail and graupel fields (Figs. 11 and 12 of Farley 1987). During the following 12 min (69–81 min simulation time), the energy flow is higher in the natural case: a sharp increase is followed by a slow decrease. In the CO_2 case this peak is smaller. Differences are negligible after 81 min simulation time. The delay-time duration of about 10–12 min and the effect-time duration of about 15 min is in the same range as the corresponding durations used in our tests. (A comparison of delay times, however, is not necessarily meaningful because the delay is strongly dependent on the manner in which seeding is conducted.)

Farley favors on the base of his model results a hypothesis (premature rainout hypothesis) that is rather distinct from the beneficial embryo competition hypothesis: seeding accelerates the development of precipitating particles that fall out before they can serve as hail embryos. This leads to a reduction of hail production without the need of the existence of a BDZ. Thus, one could speculate that the premature rainout hypothesis is responsible for the observed first rocket seeding effect. Based on the discussion in the last section, severe doubts on this hypothesis are raised in the case of the analyzed hailclouds presented here. The main difference between the Farley simulation and the Grossversuch IV seeding procedure is the development stage of the hail cloud (feeder cell versus main updraft). Further clarification on this point could be obtained by a similar numerical simulation of the Swiss-type hailclouds.

Farley found a more prominent effect on the spatial distribution of hail: seeding led to a redistribution of hail on the ground. Graupel and hail occurred in a lower concentration than in the natural case: this is possible when the amount is reduced over the same area or when the same amount is spreaded over a larger area. The latter was also indicated by the ground measurements with hailpads in Grossversuch IV [but was statistically insignificant (Federer et al. 1986, Tables 11 and 12)]. A similar result, even if statistically insignificant, was obtained by Schmid (1989) for the logarithm of the area of the 46-dBZ contour line. Unfortunately, the response variable defined in section 2 (hail kinetic energy) is not sensitive to such an effect.

Farley concludes that changes of precipitation and fallout induced by seeding may alter the dynamics of the storm. Altered dynamics can serve as an alternative explanation for the result of Schiesser et al. (1992). Instead of considering earlier freezing of melted graupel or shedded water by seeding with additional rockets to be important for the increase of the total hail kinetic energy, one may assume that this is due to aftereffects of the first (or first few) rockets. Therefore, one may also put the first rocket effect in relation to a direct microphysical impact, whereas the overall increase of hail kinetic energy during a life cycle of a storm may be due to a dynamical impact of seeding.

5. Conclusions

The first rocket effect shown graphically in Fig. 1 was statistically tested by a specially designed randomization test. Always keeping in mind the exploratory character of this study, the low p values in Table 2 are a strong hint rather than statistical proof that the effect did not occur by pure chance. The lowest p value of 0.2% is achieved when a delay time of 8 min and an effect time of 10 min is assumed (without prediction).

Microphysical considerations show that the Grossversuch IV seeding hypothesis, which assumes the existence of a BDZ, is not an adequate explanation for the first rocket effect. It is concluded from radar measurements of recent case studies of central European thunderstorms that large supercooled raindrops may occur also in the analyzed storms. But as shown in Waldvogel et al. (1987), it is unlikely that any significant number of big supercooled drops existed in the target area of the first rocket at the time when seeding was conducted.

A comparison with a model simulation from Farley (1987) shows that an effect-time duration of about 10 min agrees well with the duration of the seeding effect simulated in his model (10–12 min). Based on the model results, Farley favors the premature rainout hypothesis. Because in Grossversuch IV seeding is conducted in the main updraft when already larger reflectivities occur—and not in the feeder cell—it is concluded that the premature rainout hypothesis also does not explain the first rocket effect. A different hypothesis is given assuming introducing artificial ice nuclei leads to a significant augmentation of the number of hail embryos that compete for the available liquid water. The slower growing ice particles reach the critical size to fall later, and the consequence is that the reflectivity on the levels below the seeding zone is lower for a while than in the unseeded cases.

Acknowledgments. The authors are grateful to Dr. H. H. Schiesser for many discussions and critical comments during the course of this analysis. A referee has given helpful comments.

APPENDIX

Details of the Randomization Test

First restrict attention to a single block b that contains the $n_b = n_{0b} + n_{1b}$ cells $l_b + k$, $k = 1, \cdots, n_b$. (For block $b = 4$, consisting of cells $i = 16, 17, 18, 19$, we have $l_b = 15$, $n_b = 4$.) Let Π^* be a permutation of the numbers $[1, 2, \ldots, n_b]$ such that the $\Pi^*(k)$-th cell in block b has actually been seeded at time $\sigma_k = \sigma_j(b, k)$, $k = 1, \cdots, n_{1b}$ (usually $k = 1, 2$). [For block 4, Π^* can be chosen as the identity, $\Pi^* = (1, 2, 3, 4)$, and $\sigma_1 = 3$, $\sigma_2 = -1$.] For any permutation Π, let

$$Y_b^{(s)}(\Pi) = \sum_{k=1}^{n_{1b}} Y_{l_b+\Pi(k)}(\sigma_k),$$

$$Y_b^{(n)}(\Pi) = \sum_{k=1}^{n_{1b}} [\Sigma_i\, Y_i(\sigma_k)] - Y_b^{(s)}\Pi, \quad \text{(A1)}$$

where Σ_i is the sum over all i in block b. The test statistic

$$T_b(\Pi) = 1/n_{1b} Y_b^{(s)}(\Pi) - 1/[n_{1b}(n_b - 1)] Y_b^{(n)}(\Pi) \quad \text{(A2)}$$

for $\Pi = \Pi^*$ is the difference between the mean of Y values for actual seeding events and the mean over all

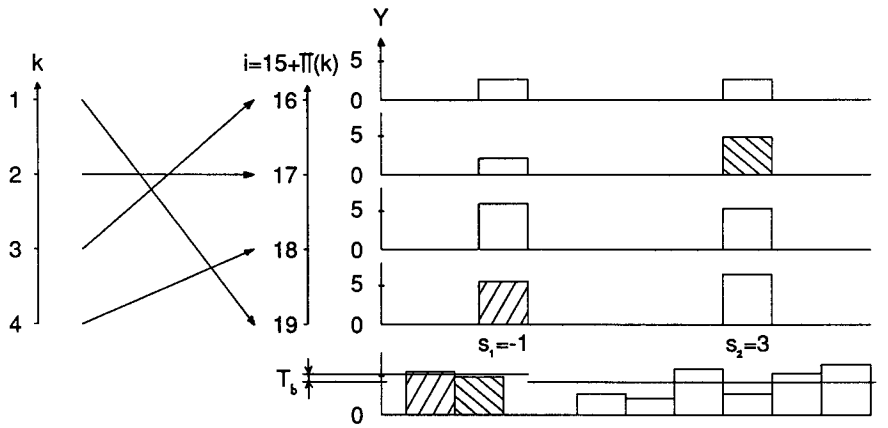

FIG. A1. Definition of the test statistic for block 4.

other potential seeding events in block b. The definition is illustrated schematically in Fig. A1 for block 4, which has $n_{0b} = 2$ unseeded cells and $n_{1b} = 2$ seeded cells.

The randomization distribution $\mathcal{L}_b$ within block b is obtained by choosing a random permutation Π in (A1). Note that the test statistic only depends on the first n_{1b} elements of the permutation Π. The number of distinct randomizations in block b is therefore $(n_{1b} + n_{0b})!/n_{0b}!$, which is equal $(2 + 2)!/2! = 12$ for block 4. This number is small enough that the randomization distribution can be obtained exactly by enumeration. Since $T_b(\Pi)$ is a linear transformation of $Y_b^{(s)}(\Pi)$, both test statistics yield the same p value p_b.

Having defined randomizations for each block, they are combined into a randomization for the whole experiment by chosing an independent randomization in each block. If the overall test statistic T is chosen to be the sum of the within-block statistics T_b, the overall randomization distribution is the convolution of the $\mathcal{L}_b$ (that is, the distribution of independent random variables with distributions $\mathcal{L}_b$). Note that any other way of combining the six independent within-block tests could have been chosen. We opted for the summation of test statistics because it seemed natural in this context.

Remark. Note how a surrogate of seeding times for unseeded cells is generated in the prescription. The seeding times realized for the seeded clouds are used to determine "pseudo" seeding times for unseeded clouds. Alternatively, one could think of simulating a rocket time for each unseeded cell, calculating the response variable for the respective effect times, and defining a randomization as the random selection of n_{b1} nominally seeded out of the $n_{b0} + n_{b1}$ cells of block b. However, if the simulation would not adequately reflect the process that led to actual seeding times, this could cause a spurious significance of the test.

REFERENCES

Farley, R. D., 1987: Numerical modeling of hailstorms and hailstone growth. Part III: Simulation of an Alberta hailstorm—natural and seeded cases. *J. Climate Appl. Meteor.*, **26,** 789–812.

Federer, B., A. Waldvogel, W. Schmid, F. Hampel, E. Rosini, D. Vento, P. Admirat, and J. F. Mezeix, 1978/79: Plan for the Swiss randomized hail suppression experiment: Design of Grossversuch IV. *Pure Appl. Geophys.*, **117,** 548–571.

——, ——, ——, H. H. Schiesser, F. Hampel, M. Schweingruber, W. Stahel, J. Bader, J. F. Mezeix, N. Doras, G. d'Aubigny, G. DerMegreditchian, and D. Vento, 1986: Main results of Grossversuch IV. *J. Climate Appl. Meteor.*, **25,** 917–957.

Höller, H., P. F. Meischner, V. N. Bringi, and J. Hubbert, 1991: Hailstorm observation by multiparameter radar. *Proc. 25th Conf. Radar Meteor.*, Paris, Amer. Meteor. Soc., 713–716.

Meischner, P. F., V. N. Bringi, D. Heimann, and H. Höller, 1991: A squall line in southern Germany: Kinematics and precipitation formation as deduced by advanced polarimetric and Doppler radar measurements. *Mon. Wea. Rev.*, **119,** 678–701.

Schiesser, H. H., J. Bader, and A. Waldvogel, 1992: Further results of Grossversuch IV: The seeding event approach. (submitted).

Schmid W., 1989: Quantitative predictions of hail intensity. *Proc. Fifth WMO Scientific Conf. on Weather Modification and Applied Cloud Physics,* Peking, World Meteor. Org., 377–380.

Waldvogel, A., and H. H. Schiesser, 1985: Time evolution of seeded hail cells in Grossversuch IV. *Proc. Fourth WMO Scientific Conf. on Weather Modification,* Honolulu, World Meteor. Org., 541–546.

——, L. Klein, D. J. Musil, and P. L. Smith, 1987: Characteristics of radar-identified big drop zones in Swiss hailstorms. *J. Climate Appl. Meteor.*, **26,** 861–877.